particular, mixing of the incoming distorted optical signal with a local light source creates a clean idler wave with information replicated from the incoming optical signal.

In the first approach, the input signal at 1,552 nm acts as the pump wave and is input to the silicon nanowaveguide along with a continuous-wave probe at 1,546 nm. The idea behind this approach is that whenever both pump and probe wave are present in silicon simultaneously, an idler wave is generated at 1,558 nm. As the efficiency of FWM is intensity dependent, a strong idler wave is generated only when the incoming optical bit has a high intensity. When the pump intensity is low, the background noise does not contribute to the generation of the idler wave. As a result, the proposed technique inherently suppresses the low-intensity noise components along with low-intensity tails of the optical signal, copying only the high-intensity optical bits to the idler. The experiment shows a 4.2-dB enhancement (about a factor of three) in the signal extinction ratio at less than 100 mW peak pump intensity. As the incoming signal is being used as the pump of the FWM process and the probe is a continuous wave, all of the timing information is copied into the idler. As a result, this technique falls short of providing timing-jitter reduction.

To provide timing-jitter reduction as well as improving the extinction ratio, the continuous-wave probe is replaced by a pulsed optical clock, which is frequency and phase synchronized to the incoming data signal. As a result, the generation of an idler wave, which carries the regenerated signal, will be controlled by the overlap between pump and probe pulses. Assuming that the clock generator is well designed with a fixed data rate, the timing jitter on the incoming optical data can be filtered by the FWM process. Similar to the first method, the multiplication of data and clock bits will generate an idler bit. As, only those data bits with high intensities can contribute to the generation of the idler, the FWM process will crop the tails of the incoming data bits and low-intensity noise components and provide a compressed and high-extinction-ratio idler wave with low timing jitter. Timing jitter can be reduced further if the optical clock is used as the pump by swapping the pump and the probe wavelengths at the input. However, in this configuration, an exact amplitude replica of the probe wave will be copied to the idler without improving the extinction ratio.

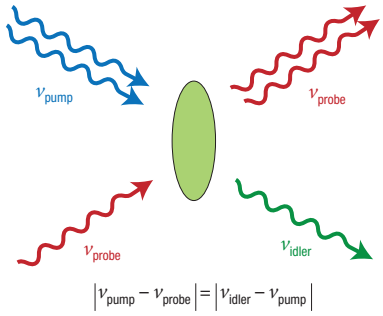

Figure 2 Four-wave mixing explained. The intensity dependence of the refractive index facilitates the mixing of two pump waves and a probe wave to amplify the probe wave by one photon and produce an idler wave, a mirror image of the probe with the opposite phase. ν represents the frequency of the corresponding optical wave.

In summary, these techniques provide a low-cost, chip-scale solution to all-optical regeneration and show that silicon photonics has a bright future ahead for real-life applications. Future work may start with addressing how the requirement for synchronization can be avoided and how bit-rate transparency can be provided. In addition, as the current configuration provides channel-by-channel regeneration, the configuration should be updated for use with multichannel communication systems.

References

1. Salem, R. *et al. Nature Photon.* **2,** 35–38 (2008).
2. Leclerc, O. *et al. Electron. Lett.* **35,** 730–731 (1999).
3. Su, Y. *et al. Proc. Optical Fiber Commun. Conf.* **MG4,** 1–3 (2001).
4. Wolfson, D. *et al. IEEE Photon. Technol. Lett.* **12,** 332–334 (2000).
5. Arahira, S. & Ogawa, Y. *IEEE Photon. Technol. Lett.* **17,** 992–994 (2005).
6. Boyraz, O. & Jalali, B. *Opt. Express* **12,** 5269–5273 (2004).
7. Rong, H. *et al. Nature* **433,** 725–728 (2005).
8. Boyraz, O. & Jalali, B. *IEICE Electron. Express* **1,** 429–434 (2004).
9. Foster, M. A. *et al. Nature* **441,** 960–963 (2006).
10. Foster, M. A. *et al. Opt. Express* **15,** 12949–12958 (2007).
11. Tien, E.-K. *et al. Opt. Express* **15,** 6500–6506 (2007).

MICROSCOPY

Brillouin bioimaging

Researchers at Harvard Medical School have developed a highly sensitive microscope that can image the mechanical properties of living tissues.

Peter So

is in the Department of Mechanical Engineering and Biological Engineering at the Massachusetts Institute of Technology, 77 Massachusetts Avenue, Cambridge, Massachusetts 02139, USA.

e-mail: ptso@mit.edu

Changes in tissue can often be a symptom of disease in the body. For example, coronary disease is accompanied by the loss of elasticity in arterial walls, fibrosis is marked by the hardening of the liver, osteoporosis involves weakening of the skeleton, and the calcification of some tissues can indicate the onset of cancer. Aside from indicating disease onset, the physical properties of tissues also regulate a variety of normal biological functions. The mechanical stress exerted by muscle-like cells initiates wound closure, for example, and compressive forces are crucial for the functioning of cartilage cells.

Clearly, the ability to map the rheological characteristics — that is, mechanical properties such as elasticity and viscosity — of biological tissues *in vivo* is important. The latest work from Giuliano Scarcelli and Seok Hyun Yun, described on page 39 of this issue[1], reports a new optical method — Brillouin microscopy — that can measure the viscoelastic properties of biological tissues, *in vivo* and non-invasively, with microscopic resolution.

Brillouin light scattering is an inelastic process that occurs when light interacts with density fluctuations in a medium. These spontaneous fluctuations are driven by collective acoustic vibrational modes (phonons) within the medium. Brillouin scattering is similar to Raman scattering, a well-known effect exploited by those working in the field of biophotonics. Raman

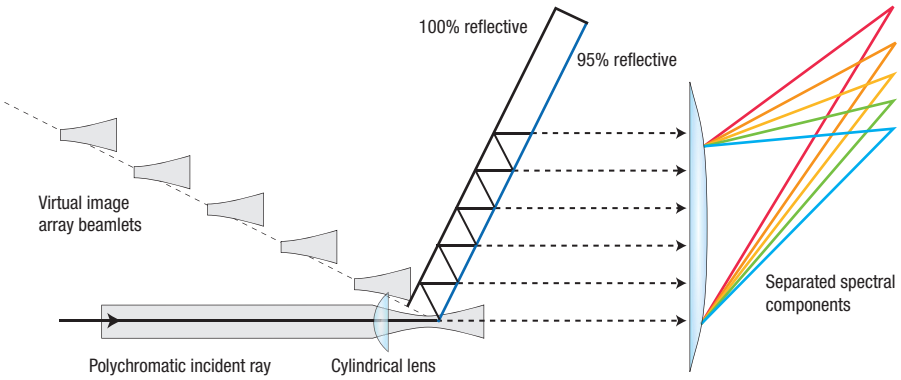

Figure 1 Schematic of a VIPA.

scattering describes the process by which incoming photons are scattered off higher energy phonons, inducing large frequency shifts in the light that can be used to characterize the intramolecular vibrational modes of the medium being probed. Brillouin scattering, on the other hand, results from photons interacting with lower energy, thermally excited acoustic phonons in a material.

Brillouin spectroscopy measures spectral changes on scattering, yielding information on the phonon's properties and therefore the viscoelastic characteristics of the medium. A major challenge for this technique is to effectively isolate Brillouin scattered photons from stronger elastically scattered signals (light from Rayleigh and Mie scattering, for example), which can be orders of magnitude stronger. Unfortunately, the frequency shifts associated with Brillouin scattering are of the order of gigahertz, which is too small to resolve with conventional spectrometers.

Traditionally, this spectral separation is accomplished through the use of high-finesse scanning Fabry–Pérot interferometers or angle-dispersive etalons (based on multiple beam interference between two parallel mirrors or plates). However, for the purposes of biomedical imaging, these devices are either too slow in terms of imaging speed, or too lossy to afford a satisfactory signal-to-noise ratio. Scarcelli and Yun have overcome these obstacles by developing a custom-built spectrometer based on a virtually imaged phase array (VIPA). The spectrometer is then integrated into a reflected-light confocal microscope.

Confocal microscopy is an imaging technique that has gained a great deal of popularity in recent years, and is promising for visualizing both static and living cells and tissues. Confocal microscopes essentially image only one point of a sample at a time, with the result that out-of-focus background light (fluorescence) is rejected in an efficient manner, thus providing three-dimensional resolution. Confocal Brillouin microscopy has remained a point sampling method mainly because the measurement times to acquire whole images have been too long (on the order of minutes per pixel).

Scarcelli and Yun extend the Brillouin technique from point sampling to a full three-dimensional imaging approach using VIPAs, which were first developed for wavelength-division multiplexing[2]. Virtually imaged phase arrays are based on a relatively straightforward concept, as presented in Fig. 1. Consider a cylindrical lens that focuses a ray of monochromatic light onto a glass plate through a slit opening in its coating. The plate is fully reflective on one side and partially (about 95%) reflective on the other. As the incident light beam undergoes multiple reflections inside the plate, the transmitted light forms a 'virtual' array of beamlets with their beam waists lined up along the plate's surface normal. These beamlets interfere to form a diffracted, collimated beam with the diffraction angle satisfying the Bragg condition. For light composed of several wavelengths, the different spectral components are diffracted over a range of angles and the VIPA disperses all wavelengths at the same time. A typically angle-dispersive etalon, in comparison, transmits a narrow band at a specific incident angle of the beam. The VIPA thus enables very efficient spectral separation that has significantly higher throughput than a typical etalon.

By integrating a VIPA into a confocal Brillouin microscope, Scarcelli and Yun report detection efficiencies that are nearly 100 times better than those obtained with point-sampling Brillouin spectroscopy techniques. Their VIPA spectrometer has a high finesse (up to 56) and large throughput efficiency over 80%, with a free spectral range of 33.3 GHz. Using this system, the researchers obtain the first cross-sectional Brillouin images that use the elastic properties of tissue as the contrast mechanism. They successfully map and quantify the dynamic crosslinking process in a polymer melt, and obtain a cross-sectional image of an acrylic lens designed for implantation. Moreover, they report the first *in situ* measurement of the elastic modulus of a crystalline lens removed from a real mouse eye.

Although this instrument has excellent potential for biomaterial characterization, there are several limitations. First, as Brillouin scattering couples photons to supersonic phonons in the material, the measured hypersonic rheological properties cannot be expected to agree with the static elastic and viscous moduli of the material. The rheological properties of many materials, especially biological ones, exhibit a complicated dependency on the mechanical perturbation frequency[3,4]. This frequency dependence cannot be detected by Brillouin microscopy because this technique probes mechanical responses only in the megahertz and gigahertz frequency ranges. However, the acoustic phonon-related rheological parameters can be readily used for comparative material characterization, such as differentiating normal and malignant tissues in disease diagnosis.

Second, the device presented here uses a low-numerical-aperture (-NA) lens, which limits the spatial resolution attainable. At present, the three-dimensional resolution of the microscope is a rather modest 6 μm (x direction) by 6 μm (y direction) by 60 μm (z direction). Although resolution can be improved by increasing the NA of the lens, a high NA (exceeding 0.5) leads to noticeable Brillouin line broadening resulting from the dependence of the frequency shift on the light scattering angle, and also reduces the acousto–optical interaction length, which determines the signal strength of the Brillouin scattered light. These resolution limitations restrict the ability to fully characterize biomedically important systems such as arterial walls, which have stratified structures with layer thicknesses on the order of tens of micrometres. Overcoming this issue will be an important future challenge.

Finally, the performance of the microscope has only been demonstrated in relatively transparent specimens. The definitive biomedical demonstration of this technique awaits future comparative measurements of normal versus pathological tissues that are typically more opaque.

References

1. Scarcelli, G. & Yun, S. H. *Nature Photon.* **2,** 39–43 (2008).
2. Shirasaki, M. *Opt. Lett.* **21,** 366–368 (1996).
3. Deng, L. *et al. Nature Mater.* **5,** 636–640 (2006).
4. Bao, G. & Suresh, S. *Nature Mater.* **2,** 715–725 (2003).